

Predicting Movement of the Warm Pool, the Salinity Front, and the Convergence Zone in the Western and Central Part of Equatorial Pacific Using a Coupled Hydrodynamical-Ecological Model

Supangat¹, A., T. Rameyo Adi¹, Widodo S. Pranowo¹, and N.S. Ningsih².

¹Agency for Marine Affairs and Fisheries, Indonesia

²Study Program of Oceanography, Bandung Institute of Technology, Indonesia

ABSTRACT

A coupled hydrodynamical-ecological model for regional and shelf seas called 'COHERENS' and developed by Luyten *et al.* (1999) was used to predict the water dynamics, distribution of temperature and salinity in the western and central part of equatorial Pacific. The model results have demonstrated well equatorial processes that exist in the ocean, such as the major currents, the western equatorial Pacific warm pool, equatorial upwelling in the central Pacific, and the permanent convergence of surface-layer water masses on the eastern edge of the warm pool. Lehodey *et al.* (1997) published that one of the most successful fishing grounds is located in the vicinity of the convergence zone between the warm ($> 28 - 29^{\circ}\text{C}$) low-salinity water of the warm pool and the cold saline water of the central Pacific equatorial upwelling. This zone of convergence, identified by a well-marked salinity front and approximated by the $28 - 29^{\circ}\text{C}$ sea surface temperature (SST) isotherm, has been simulated well by the model. Therefore, seasonal variations of movement of the $28 - 29^{\circ}\text{C}$ isotherm, the salinity front, and the convergence zone are important to be predicted. We would expect that the model results might be able to be used for the prediction of good fishing grounds.

Key Words: coupled-models, major currents, warm pool, equatorial upwelling, convergence zone, salinity front, Pacific, fishing grounds.

INTRODUCTION

The basic feature and the existence of equatorial processes in the Pacific Ocean, such as the major currents, the western equatorial Pacific warm pool (WEPWP, defined by sea surface temperatures $\geq 28^{\circ}\text{C}$), equatorial upwelling in the central Pacific, and

the permanent convergence of surface-layer water masses on the eastern edge of the warm pool, have been documented by previous scientists (e.g., Tomczak and Godfrey, 1994; Wyrtky, 1989; Stewart, 2002). Understanding the spatial and temporal evolution of the equatorial processes is an important factor for atmospheric circulation and fisheries.

Stewart (2002) summarized characteristics of the equatorial processes in the Pacific Ocean, as follows: (i) there are permanent major currents in the equatorial Pacific (e.g., the wind-driven North and South Equatorial Currents, North and South Equatorial Counter Current, Equatorial Under Current, and Equatorial Intermediate Current), (ii) surface waters are warmest in the WEPWP, (iii) the divergence of the Ekman transport produces upwelling of cold water on the equator, and (iv) there is a permanent convergence of surface-layer water masses on the eastern edge of the warm pool that is close to cold tongue of water around the equator.

It has been recognized that the major currents in the equatorial Pacific redistribute heat, which is then released by the rain. The released heat, variability of currents and temperatures in the equatorial region plays an important role in the atmospheric circulation (Stewart, 2002). In addition, movement of the WEPWP has been the subject of intense researches recently because it is related to the development of ENSO (El Niño Southern Oscillation) events and the earth's climate in general (Philander, 1990; Wyrtky, 1989; Yan *et al.*, 1997). Meanwhile, Lehodey *et al.* (1997) published that nearly 70 % of the world's annual tuna harvest comes from the Pacific Ocean, in which catches are highest in the WEPWP. In addition, they also reported that one of the most successful fishing grounds is located in the vicinity of the convergence zone between the warm ($> 28 - 29^{\circ}\text{C}$) low-salinity water of the warm pool and the cold saline water of the central Pacific equatorial upwelling. This zone of convergence is identified by a well-marked salinity front and approximated by the $28 - 29^{\circ}\text{C}$ sea surface temperature (SST) isotherm.

The equatorial processes respond quickly to variations in the wind fields, mainly the Trade winds (the northeastern and southeastern Trades), which are highly persistent winds converging near the equator in a narrow Intertropical Convergence Zone. Previous scientists have documented that although the Trades are remarkably steady, they do vary from month to month and can change dramatically from year to year (e.g., Tomczak and Godfrey, 1994; Wyrtky, 1989; Stewart, 2002). Therefore, the strength and position of the equatorial currents and upwelling vary both seasonally associated with meridional variations of sunlight and annually associated with the ENSO phenomenon. In addition, the warm pool, the salinity front, and the convergence zone also move both seasonally and annually.

In the present study, we address to predict seasonal variations of the equatorial processes, such as strength and position equatorial currents and upwelling, and movement of the warm pool, the salinity front, and the convergence zone in the western and central part of equatorial Pacific by using numerical model. A coupled hydrodynamical-ecological model called 'COHERENS' and developed by Luyten *et al.* (1999) was used to predict the water dynamics, distribution of temperature and salinity in the western and central part of equatorial Pacific. For sake of simplicity and as a preliminary study, we neglected interannual variability of the equatorial processes although it has been documented by previous scientists (e.g., Tomczak and Godfrey, 1994; Wyrky, 1989; Stewart, 2002).

MODEL CONFIGURATION

A three-dimensional prognostic calculation of the COHERENS was used in this study. Location of the study area is from of 20 °S - 20 °N, and 120 °E -150 °W. The domain is covered by 181 x 81 grid cells at approximately 0.5° resolution. The vertical grid consists of 19 σ -levels concentrated over the upper and intermediate depths in order to adequately resolve the respective wind-influenced layers. The bathymetry was interpolated from the GTOPO30 data set (http://topex.ucsd.edu/cgi-bin/get_data.cgi). The external and internal mode time steps used in the simulation are 60 s and 1200 s, respectively. The main forcing for the model is the 5 daily-wind fields derived from SSM/I (Special-Sensor Microwave/Imager), PODAAC (Physical Oceanography Distributed Active Archive Center). The initial temperature and salinity data are taken from the Levitus data (1982). In addition to the wind field data, the following surface data were supplied to the model, namely monthly mean values of air temperature, atmospheric pressure, relative humidity, cloud coverage, evaporation and precipitation rates, which are derived from DASILVA (<http://Ingrid.ldeo.columbia.edu/SOURCE/.DASILVA>). The simulations covered a full yearly cycle for the year 1993 providing a prediction of monthly averaged fields of the equatorial processes.

Results and Discussion

MAJOR CURRENTS IN THE EQUATORIAL PACIFIC

The model results reproduce well the existence of permanent major currents in the equatorial Pacific. Monthly averaged surface distributions of currents and temperature during 1993 are shown in Fig. 1. The figure shows the major westward components of the equatorial current system, namely the North and South Equatorial Current (NEC and SEC, respectively). It can be seen that the NEC and SEC vary seasonally in

strength. The NEC flows steadily during the whole year between 8 °N and 15 °N with speeds of 0.5 m s⁻¹ or less. In the northern winter, the NEC seems to be stronger, for example in January and December (Fig. 1). During the month of April 1993 (weak event of El Niño), the NEC remained strong and it reached speeds of 0.5 m s⁻¹. Meanwhile, the strength of NEC was reduced in the northern summer (i.e., in July and August) and during the months of September and October with speeds of 0.2 m s⁻¹ or less. On the other hand, the SEC was very weak in January and increased afterwards gradually until it is most strongly developed in April with speeds of 1.0 m s⁻¹ or less. In addition, in the month of April, the SEC extends so far to the northern hemisphere reaching 3 °N. Meanwhile, during the month of July and October, the SEC was still developed. However, its strength decreased and its position moved further south around 6 - 13 °S.

The simulations also shows the most important eastward flow in the equatorial current system, namely the North Equatorial Counter Current (NECC) and the Equatorial Under Current (EUC), as shown in Fig. 1 and 2, respectively. The NECC is strongly seasonal, in which in May it starts to be fed from both hemispheres, flows between 2 - 7 °N, and reaches its greatest strength during July – December with speeds of 0.7 m s⁻¹ or less (Fig. 1). Meanwhile, during January – April the NECC is weak and flows around 2 - 5 °N. According to Tomczak and Godfrey (1994), during the months of January – April, the Northwest Monsoon prevents the SEC from feeding the NECC, so that the strength of NECC was reduced (Fig. 1).

Figure 2 shows simulation results of monthly averaged zonal velocity at 170 °W for January, April, July, and October 1993. The existence of the EUC below the surface on the equator can be seen in the figure. The EUC flows strongest during February – July but it is much weaker in August – January. In the month of January, the EUC is very weak at speeds of 0.05 m s⁻¹ or less. This may be due to a weakening of the SEC in January. Tomczak and Godfrey (1994) concluded that the EUC belongs entirely to the southern circulation system and its source waters originate mainly from the southern hemisphere. In addition, they reported that the EUC is fed from the SEC. Therefore, the EUC is associated with variable strength of the SEC. In this study, the core of EUC is found at a depth of from 300 to 600 m. Meanwhile, according to Tomczak and Godfrey (1994), its existence is found at 200 m depth. An explanation for the difference of results obtained from both studies is still lacking. A good explanation might be obtained by extending the simulation periods, which represent periods of marked interannual variations in the equatorial Pacific (i.e., associated with the El Niño and La Niña phenomena). Existence of the Equatorial Intermediate Current (EIC), flowing from East to West, is also found by the model (Fig. 2). The current core is found at a depth of from 900 to 1900 m.

WESTERN EQUATORIAL PACIFIC WARM POOL

Figure 1 also shows monthly averaged spatial distribution of the western equatorial Pacific warm pool (WEPWP), which is defined by sea surface temperatures $\geq 28^{\circ}\text{C}$ during 1993. The spatial and temporal movement of the warm pool can be seen in the figure. During the months of January – April, the WEPWP mainly existed in the southern hemisphere and then moved mostly northward associated with the meridional movement of the sun. Meanwhile, around the western equator the SST decreased from $\geq 28^{\circ}$ to $27\text{--}28^{\circ}\text{C}$ in June – October, and to $26\text{--}27^{\circ}\text{C}$ in November – December. It is not clear whether this decrease in temperature is due to the 1993 El Niño event or the zonal transport of cold water originating in the central Pacific equatorial upwelling by the westward-flowing south equatorial current.

EQUATORIAL UPWELLING IN THE CENTRAL PACIFIC

The existence of equatorial upwelling in the central Pacific is well indicated in Fig. 1 and identified by a cold tongue of water around the equator. During the months of January – March, a cold tongue of $26\text{--}27^{\circ}\text{C}$ reached around 167°W , and then extended further westward in April – September with a maximum distance of 160°E in July. The westward displacement is induced by the strong south equatorial current (SEC). In April, a $25\text{--}26^{\circ}\text{C}$ cold tongue started to present reaching around 173°W . The cold tongue also extended further westward during the months of May – December and reaching a maximum of 175°E in December (Fig. 1).

In addition, the presence of equatorial upwelling can be also seen in Fig. 3. The figure showed simulation results of monthly averaged temperature for January, April, July, and October 1993 along a vertical transect at 170°W . In January, the upwelling strength was weak indicated by the $27\text{--}28^{\circ}\text{C}$ isotherms, which are upwelled to the surface on the equator. In the other months, the upwelling strength increased and it was indicated by the isotherm of $26\text{--}27^{\circ}\text{C}$ in April, and of $25\text{--}26^{\circ}\text{C}$ in July and October.

CONVERGENCE ZONE AND SALINITY FRONT

Figure 4 and 5 show monthly averaged distribution of surface salinity for the months of January – June and July – December 1993, respectively. The thin solid lines indicating the 26 , 27 , 28 , and 28.5°C isotherms and the thin dash line pointing to the 34.6 isohaline are superimposed in the figures. Overlaying the cold tongue of water around the equator on the spatial distribution of surface salinity for the same month indicates that the warm low-salinity water of the warm pool would converge with the cold saline water of the central Pacific equatorial upwelling. This pattern appears to be

permanent, as shown in Fig. 4 and 5. Therefore, the major feature on this figure is the presence of a permanent convergence of surface-layer water masses on the eastern edge of the warm pool that is close to cold tongue of water around the equator. The convergence zone is identified by a well-marked salinity front and approximated by the 26 – 29 °C isotherm. Here, the salinity front is approximated by the 34.6 isohaline. The model results show the spatial and temporal evolution of the convergence zone, which moved both zonally and meridionally. Meanwhile, we also superimposed lines that represent the convergence zone in Fig.4 and 5, namely the thick solid line with arrows on the both corners (close to the 28.5 °C isotherm), the dash solid line with arrows on the both corners (close to the 28 °C isotherm), the square dot line with arrows on the both corners (close to the 27 °C isotherm), and the long dash line (close to the 26 °C isotherm).

During the months of January, February, and March, the convergence zone is identified by a well-marked salinity front and approximated by the 28 – 29 °C isotherm, as delineated on Fig. 4 by the thick solid line with arrows on the both corners. In the periods, the convergence zone appeared around 163 °E – 150 °W and 13 °S - 6 °N. In April, the convergence zone, marked by the thick and dash solid line with arrows on the both corners (close to the 28.5 and 28 °C isotherms, respectively), was found around 165 °E – 158 °W and 8 °S - 5 °N. In May, it moved further westward reaching around 156 °E and was marked by the dash solid line with arrows on the both corners (close to the 28 °C isotherm). In June – August (Fig. 4 and 5), the convergence zone existed around 162 °E – 162 °W and 13 °S - 4 °N and was marked by the dash-solid and the square-dot lines with arrows on the both corners, which close to the 28 °C and 27 °C isotherms, respectively. Meanwhile, during the months of September – December (Fig. 5), it appeared mostly in the southern hemisphere (163 °E – 164 °W and 13 °S - 3 °N) and was delineated by the square-dot lines with arrows on the both corners and by the long dash line, which close to the 27 °C and 26 °C isotherms, respectively. Meanwhile, around the western equator the SST decreased from ≥ 28 to 27- 28 °C in June – October, and to 26- 27 °C in November – December. As mentioned previously, during the months of June – December there was a decrease in temperature of WEPWP, so that we used the >26 and >27 °C isotherms to indicate the convergence zone.

As reported by Lehodey *et al.* (1997), one of the most successful fishing grounds is located in the vicinity of the convergence zone. For model verification in the present study, we used the location of US purse-seiners catch per unit effort (CPUE) data >10 mt d⁻¹ (metric tonnes per fishing day on a 1 week time resolution) of skipjack tuna, which is published by Lehodey *et al.* (1998) for the month of June 1994. The location is approximated by the ellipse shapes in Fig. 4 (for the month of June). In general, the present simulated convergence zone is in agreement with the location of high skipjack

tuna CPUE although there is a shift in space appears between them. The space shift could be due to the difference of the periods of simulation (1993) and the CPUE data (1994) and also because the surface data supplied to the model (i.e., monthly mean values of air temperature, atmospheric pressure, relative humidity, cloud coverage, evaporation and precipitation rates) are not representative. We would expect that the model results might be able to be improved significantly if we used a shorter interval of the surface data, namely at least 12-hourly data in order to represent the daytime and nighttime data.

Concluding Remarks

Equatorial processes that exist in the western and central part of equatorial Pacific Ocean (e.g., the major currents, the western equatorial Pacific warm pool, equatorial upwelling in the central Pacific, and the permanent convergence of surface-layer water masses on the eastern edge of the warm pool) have been predicted by using the three-dimensional prognostic calculation of COHERENS developed by Luyten *et al.* (1999). The model results have shown the spatial and temporal evolution of the warm pool, the salinity front, and the convergence zone. In general, during the period of simulation (1993), the convergence zone, as the one of the most successful fishing grounds, was found around 156 °E – 150 °W and 13 °S - 6 °N. The present simulated convergence zone is generally encouraging. However, to obtain a significant improvement of the predicting movement of the warm pool, salinity front, and convergence zone, it is important to extend the simulation periods in order to acquire some insight on the interannual variability of equatorial processes. In addition, to improve the model results, it is also necessary to use a shorter interval of the surface data (at least 12-hourly data), which are supplied to the model, such as values of air temperature, atmospheric pressure, relative humidity, cloud coverage, evaporation and precipitation rates. By extending the simulation periods and using the shorter interval of the surface data as well as the availability of good and complete data of skipjack tuna catch and fishing effort, we would expect to establish the link of behaviour, migration pattern, and seasonal distribution of the fish to the physical properties and variability of the water. Once the link of them are established, knowledge of climate variability and the ocean's role in the convergence zone can then be used for the prediction of good fishing grounds, namely increasing the catch, while keeping the sustainable stocks.

REFERENCES

- Lehodey, P., Bertignac, M., Hampton, J., Lewis, A. and Picaut, J. (1997) El Niño Southern Oscillation and Tuna in the Western Pacific. *Nature* 389: 715-718.
- Lehodey, P., Andre, J-M., Bertignac, M., Hampton, J., Stoens, A., Menkes, C., Memery, L. and Grima, N. (1998) Predicting Skipjack Tuna Forage Distributions in the Equatorial Pacific using A Coupled Dynamical Bio-geochemical Model. *Fish Oceanogr.* 7(3/4): pp. 1-9.
- Levitus, S. (1982) Climatological Atlas of the World Ocean. U.S. Department of

Commerce, National Oceanographic and Atmospheric Administration, Tech. Rep. 13: 173 pp.

Luyten, P.J., Jones, J.E., Proctor, R., Tabor, A., Tett, P., and Wild-Allend, K. (1999) COHERENS — A Coupled Hydrodynamical–Ecological Model for Regional and Shelf Seas: User Documentation. MUMM Report, Management Unit of the Mathematical Models of the North Sea, 914 pp.

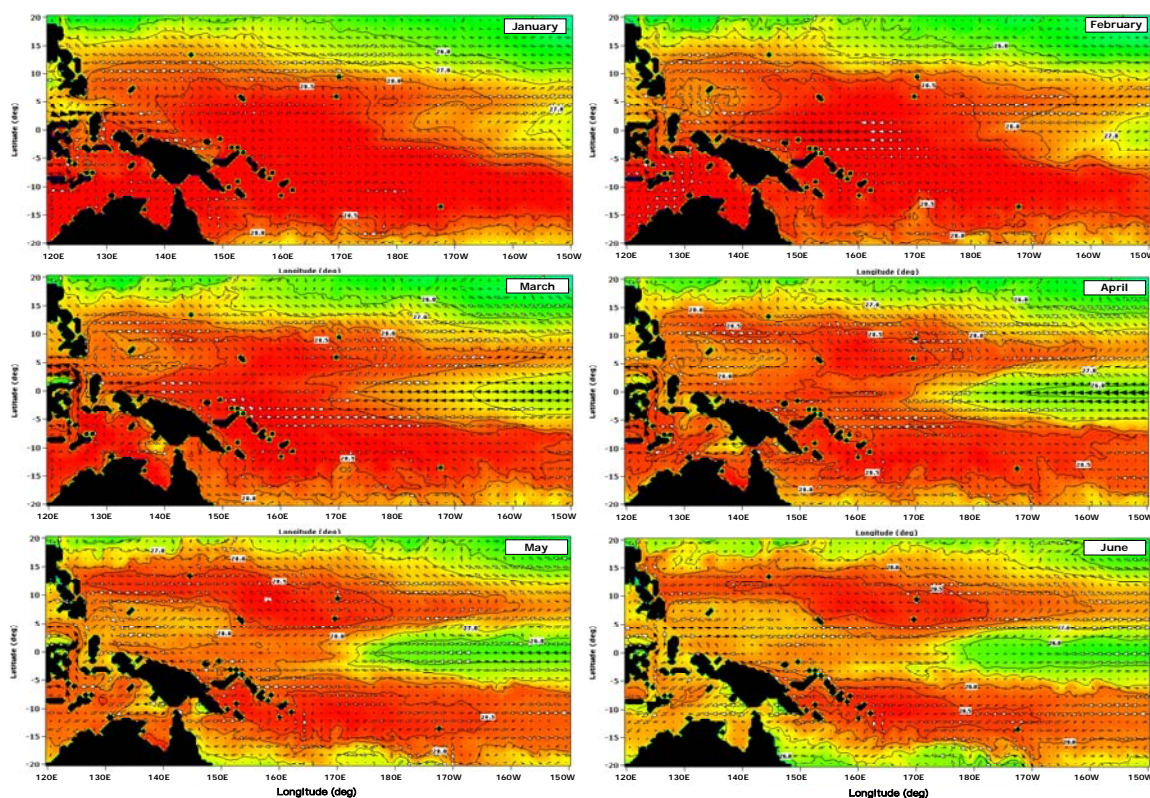
Philander, S. G. (1990) El Niño, La Niña, Southern Oscillation. Academic Press, 293 pp.

Stewart, R. H. (2002) Introduction to Physical Oceanography. Spring 2002 Edition, 341 pp.

Tomczak, M. and Godfrey, J. S. (1994) Regional Oceanography: An Introduction, Butler & Tanner Ltd, Frome and London, 422 pp.

Yan, X., He, Y., Liu, W.T, Zheng, Q., Ho, C. (1997) Centroid Motion of the Western Pacific Warm Pool during Three Recent El Niño Southern Oscillation Events. J. Phys. Oceanogr. 27: 837-845.

Wyrtki, K. (1989) Some Thoughts about the west Pacific Warm Pool. Proc. Western Pacific Int. Meeting and Workshop on TOGA COARE, New Caledonia, ORSTUM, Centre de Nouma, pp. 99-109.



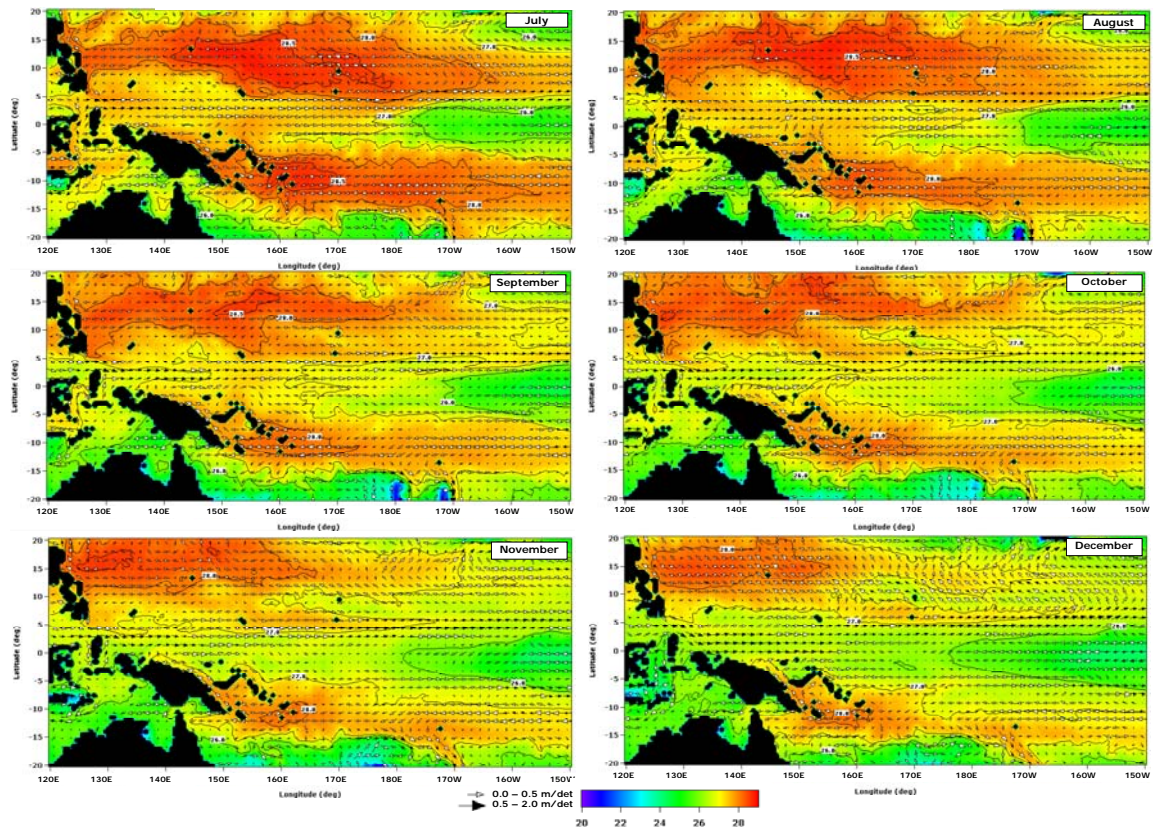


Figure 1. Monthly averaged surface distributions of currents (m s^{-1}) and temperature ($^{\circ}\text{C}$) during 1993. The contours of the 26, 27, 28, and 28.5°C isotherms are superimposed.

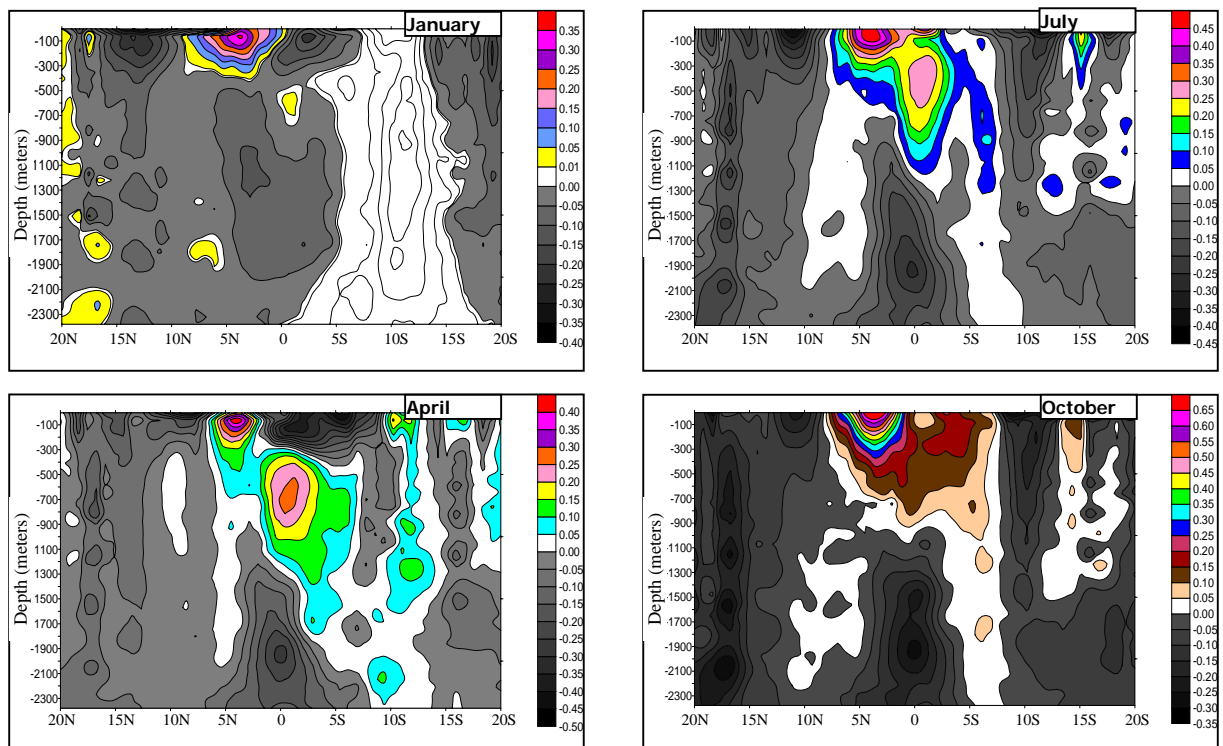


Figure 2. Monthly averaged zonal velocity (m s^{-1}) at 170°W for January, April, July, and October 1993. Positive values are eastward currents, whereas negative values are westward currents.

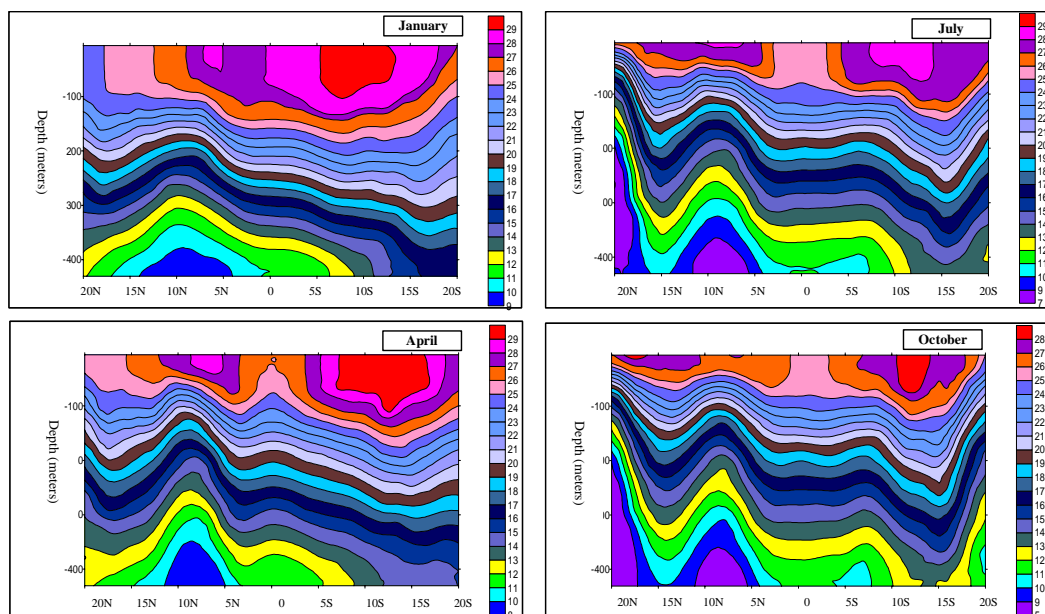


Figure 3. Monthly averaged temperature ($^\circ\text{C}$) for January, April, July, and October 1993 along a vertical transect at 170°W .

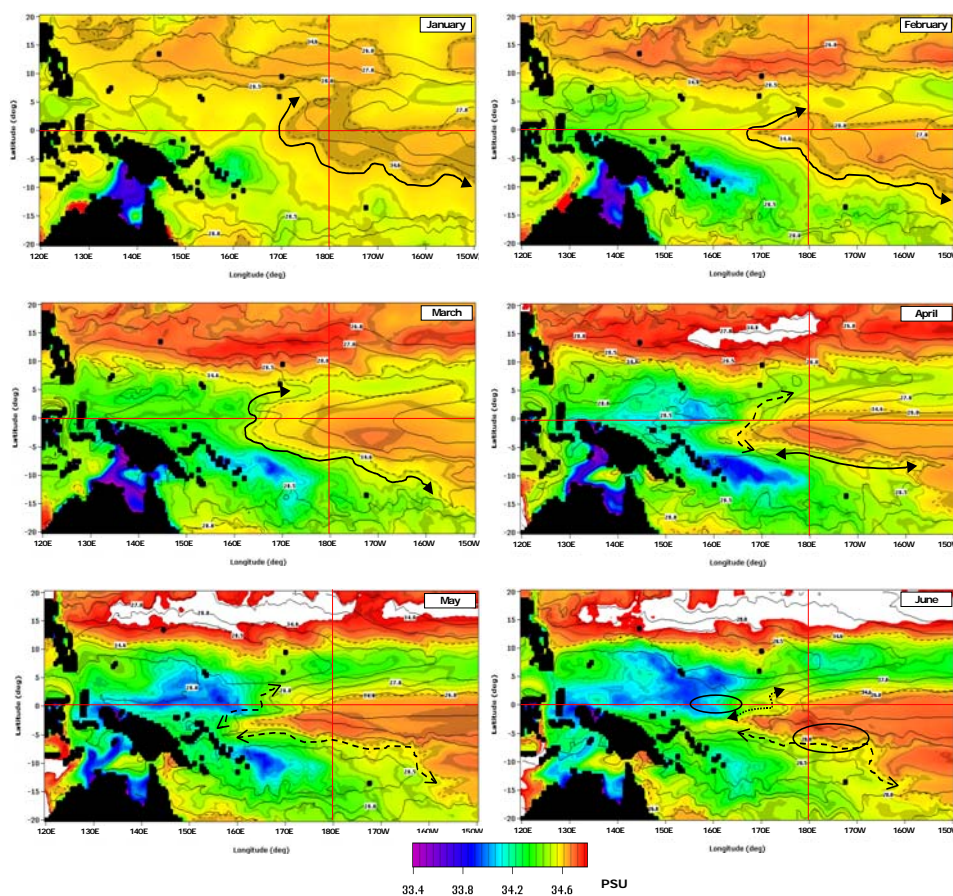


Figure 4. Monthly averaged distributions of surface salinity during the months of January – June 1993. The thin solid lines indicate the 26, 27, 28, and 28.5°C

isotherms, whereas the thin dash line is the 34.6 isohaline. The delineation of the convergence zone is approximated by the thick solid line with arrows on the both corners (close to the 28.5 °C isotherm), the dash solid line with arrows on the both corners (close to the 28 °C isotherm), the square dot line with arrows on the both corners (close to the 27 °C isotherm), and the long dash line (close to the 26 °C isotherm). For the month of June we imposed the location of US purse-seiners catch per unit effort (CPUE) data >10 mt d⁻¹ of skipjack tuna, which is published by Lehodey *et al.* (1998) and approximated by the ellipse shapes.

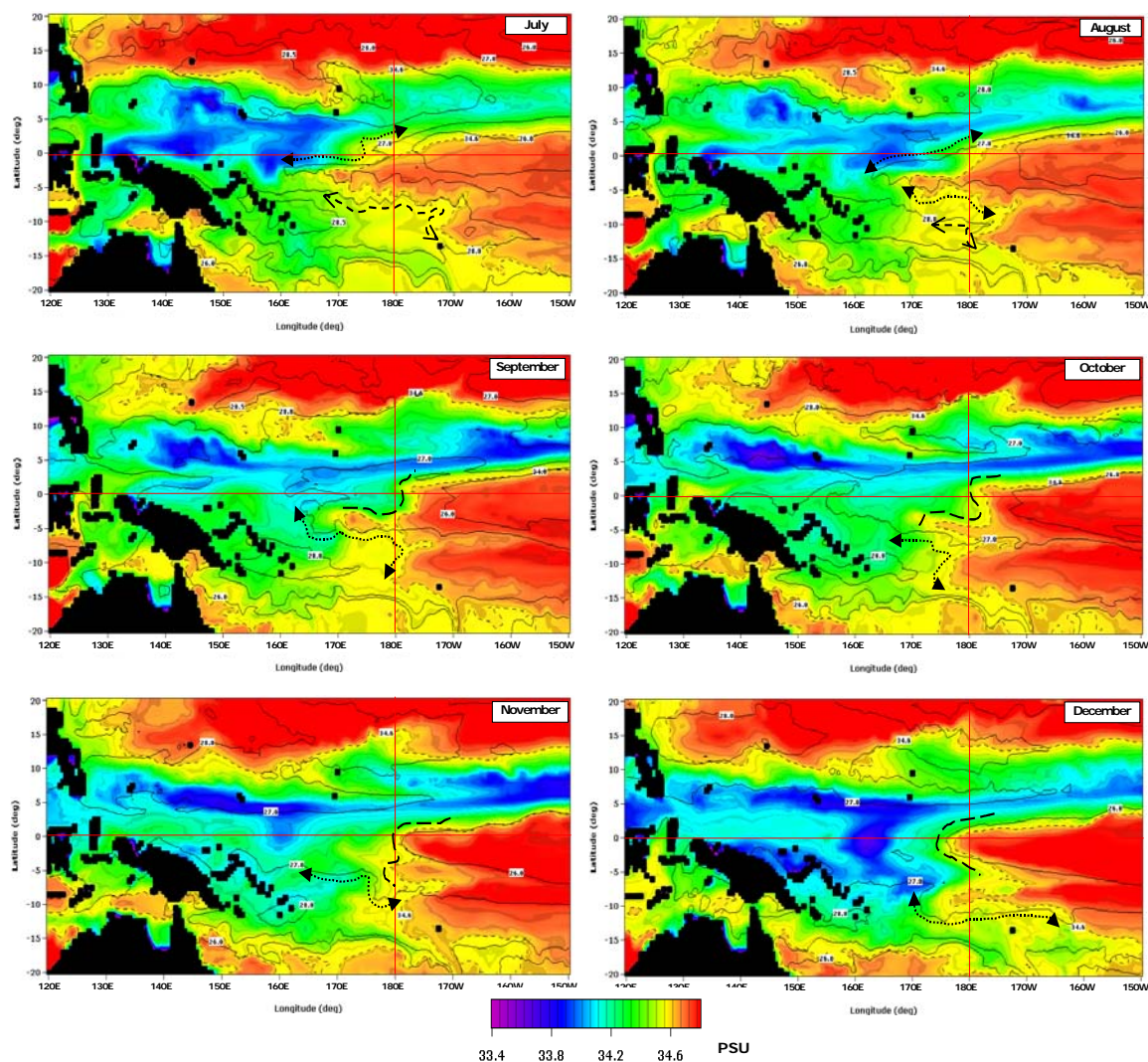


Figure 5. As for Fig. 4, except during the months of July – December 1993.